Hyperpolarized ^{129}Xenon Magnetic Resonance Imaging to Quantify Regional Ventilation Differences in Mild to Moderate Asthma

A Prospective Comparison Between Semiautomated Ventilation Defect Percentage Calculation and Pulmonary Function Tests

Lukas Ebner, MD, Mu He, MS,†‡ Rohan S. Virgincar, MS,† Timothy Heacock, MD,§ Suryanarayanan S. Kaushik, PhD,‖ Matthew S. Freemann, PhD,†¶ H. Page McAdams, MD,* Monica Kraft, MD,§ and Bastiaan Driehuys, PhD*†‖¶*

Objectives: The aim of this study was to investigate ventilation in mild to moderate asthmatic patients and age-matched controls using hyperpolarized (HP) ^{129}Xenon magnetic resonance imaging (MRI) and correlate findings with pulmonary function tests (PFTs).

Materials and Methods: This single-center, Health Insurance Portability and Accountability Act–compliant prospective study was approved by our institutional review board. Thirty subjects (10 young asthmatic patients, 26 ± 6 years; 3 males, 7 females; 10 older asthmatic patients, 64 ± 6 years; 3 males, 7 females; 10 healthy controls) were enrolled. After repeated PFTs 1 week apart, the subjects underwent 2 MRI scans within 10 minutes, inhaling 1-L volumes containing 0.5 to 1 L of ^{129}Xe. ^{129}Xe ventilation signal was quantified by linear binning, from which the ventilation defect percentage (VDP) was derived. Differences in VDP among subgroups and variability with age were evaluated using 1-tailed *t* tests. Correlation of VDP with PFTs was tested using Pearson correlation coefficient. Reproducibility of VDP was assessed using Bland-Altman plots, linear regression (R^2), intraclass correlation coefficient, and concordance correlation coefficient.

Results: Ventilation defect percentage was significantly higher in young asthmatic patients versus young healthy subjects (8.4% ± 3.2% vs 5.6% ± 1.7%, $P = 0.031$), but not in older asthmatic patients versus age-matched controls (16.8% ± 10.3% vs 11.6% ± 6.6%, $P = 0.13$). Ventilation defect percentage was found to increase significantly with age (healthy, $P = 0.05$; asthmatic patients, $P = 0.033$). Ventilation defect percentage was highly reproducible ($R^2 = 0.976$; intraclass correlation coefficient, 0.977; concordance correlation coefficient, 0.976) and significantly correlated with $FEV_{1\%}$ ($r = -0.42$, $P = 0.025$), $FEF_{25\%–75\%}$ ($r = -0.45$, $P = 0.019$), FEV1/FVC ($r = -0.71$, $P < 0.0001$), FeNO ($r = 0.69$, $P < 0.0001$), and RV/TLC ($r = 0.51$, $P = 0.0067$). Bland-Altman analysis showed a bias for VDP of −0.88 ± 1.52 (FEV1%, −0.33 ± 7.18).

Conclusions: ^{129}Xenon MRI is able to depict airway obstructions in mild to moderate asthma and significantly correlates with PFTs.

Key Words: lung MRI, hyperpolarized xenon gas, airway obstruction, asthma, pulmonary function tests

(*Invest Radiol* 2017;52: 120–127)

Asthma has a prevalence of 6% to 8% in the American population that peaks in early childhood, declines in late adolescence, and rises again in the late adulthood before decreasing among the elderly.[1,2]

While the diagnosis and clinical monitoring of asthma mainly use forced expiratory volume in 1 second (FEV1%), these pulmonary function tests (PFTs) do not completely characterize airway physiology. Even in subjects with normal FEV1%, nitrogen washout shows that significant ventilation heterogeneity can be present.[3] Similarly, computed tomography (CT) can reveal heterogeneous regional air-trapping and airway thickening in asthmatic patients[4] with normal PFT results. The most striking shortcoming of PFTs is their broad variation with age, standing height, sex, and ethnic group.[5,6] These observations support the need for more precise and reliable measurements that do not require such scaling. In addition to being highly variable, PFTs also cannot depict regional ventilation or its heterogeneity. Ventilation defects could represent preclinical stages of disease, offering the opportunity of better monitoring disease progress or treatment efficiency. Another possible application could include early detection of disease-related ventilation defects to further avoid exacerbations.[7]

To this end, xenon-enhanced dual-energy CT has been able to depict regional ventilation but confers a considerable radiation dose, which particularly limits the use in healthy subjects and young individuals.[8] Therefore, MRI techniques are emerging that use short echo time sequences in conjunction with oxygen shortening lung tissue T1 to provide a surrogate of regional ventilation.[9] Although the oxygen enhancement signal depends on more than regional ventilation, it has been shown to significantly correlate with PFT measurements. However, oxygen-enhanced MRI is hampered by relatively small signal, long acquisition times, and the need for subtraction that can make it prone to misregistration artifacts.[10]

Even more advantageous are nonproton MR methods that directly image nonendogenous inhaled agents, such as perfluorinated gases, without background signal.[11] However, the most thoroughly investigated and mature nonproton method over the last 2 decades has been hyperpolarized (HP) ^{3}He MRI.[12–15] This technique also readily depicts ventilation heterogeneity and defects and has been used to visualize the effects of both bronchoprovocation and bronchodilation.[16] The observed ventilation defects on HP ^{3}He MRI significantly correlated

Received for publication April 29, 2016; and accepted for publication, after revision, July 5, 2016.

From the *Department of Radiology, and †Center for In Vivo Microscopy, Duke University Medical Center; ‡Department of Electrical and Computer Engineering, Duke University; §Department of Pulmonary and Critical Care Medicine, Duke University Medical Center; ‖Department of Biomedical Engineering, and ¶Medical Physics Graduate Program, Duke University, Durham, NC.

L.E. and B.D. are the guarantors of the integrity of the entire study and the contributors to the literature research. All the authors contributed to the study concepts/study design, data acquisition, or data analysis/interpretation; manuscript drafting or manuscript revision for important intellectual content; and approval of the final version of the submitted manuscript. T.H. and M.K. contributed to the clinical studies. M.H., S.S.K., M.S.F., and B.D. are the magnetic resonance experiments. M.H. and R.S.V. contributed to the statistical analysis. B.D., H.P.M., and R.S.V. contributed to the manuscript editing.

Conflicts of interest and sources of funding: This study was funded by Chiesi Pharmaceuticals, with additional support from NIH/NHLBI R01 HL105643 and the Duke Center for In Vivo Microscopy, an NIH/NIBIB National Biomedical Technology Resource Center (P41 EB015897). Lukas Ebner received financial funding by the Swiss National Science Foundation (grant P2SKP3_158645/1).

B.D. is a founder of Polarean, Inc.

Correspondence to: Lukas Ebner, MD, Department of Radiology, Duke University Medical Center, 3808, 2301 Erwin Road, Durham, NC 27710. E-mail: lukas.ebner@duke.edu.

ISSN: 0020-9996/17/5202–0120
DOI: 10.1097/RLI.0000000000000322

with areas of air-trapping, resulting from airway remodeling encountered on CT.[17] ^{3}He MRI has shown that older asthmatic patients exhibit significantly more ventilation defects than younger ones.[11] Unfortunately, ^{3}He gas is in short supply and faces sharply rising costs, which has increased interest in readily available HP ^{129}Xe. This gas has already been shown to detect more ventilation defects in asthmatic patients than ^{3}He.[18] However, there are no studies further investigating obstructive patterns in asthma with ^{129}Xe MRI or correlating this technique with PFTs. This gap must be addressed in order for ^{129}Xe MRI to expand into clinical practice.

The purpose of our study was to investigate if ^{129}Xe MRI would (*a*) correlate significantly with established lung function metrics; (*b*) accurately depict differences in ventilation defect percentage (VDP) between asthmatic patients and healthy controls; and (*c*) be reproducible at baseline.

MATERIALS AND METHODS

This prospective, single-center Health Insurance Portability and Accountability Act–compliant study was approved by the institutional review board and registered at clinicaltrials.gov. All subjects gave informed, written consent before study enrollment.

Patients

Between January 2012 and March 2014, 30 subjects were prospectively recruited for this study (20 asthmatic patients, 10 age-matched healthy controls). Both study populations were matched for sex, asthma medication use, and percent predicted forced expiratory volume (FEV1%). Asthma was confirmed with a methacholine challenge test according to American Thoracic Society guidelines.[6] The population was further stratified by age to young (18-35 years; n = 9) and older (55–75 years; n = 10) asthmatic patients, and included 5 age-matched healthy subjects for each age group.

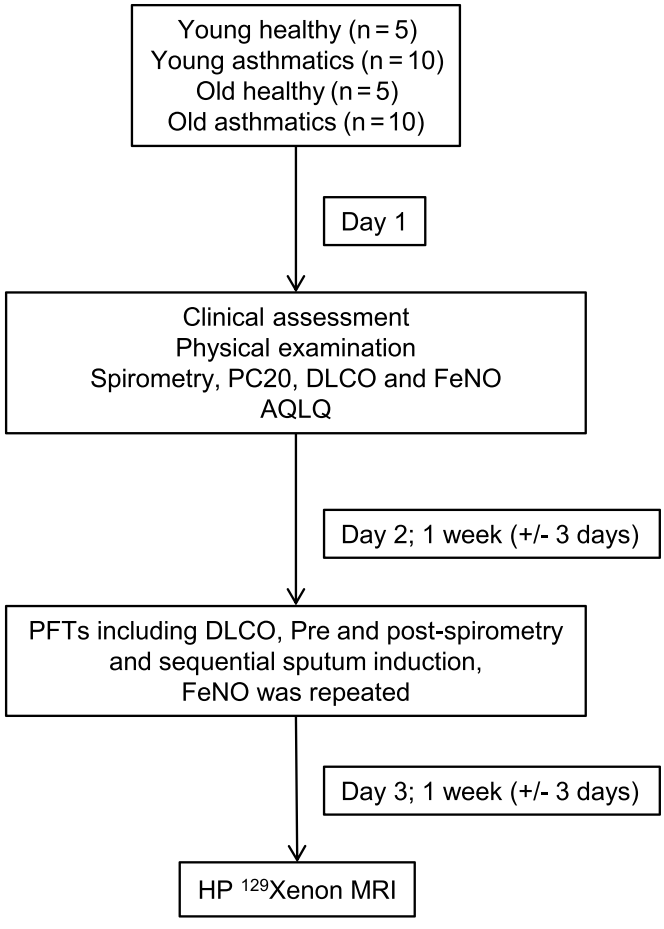

FIGURE 1. Flowchart of study recruitment and the diagnostic workup timeline.

The following exclusion criteria were applied: (1) smoking history of more than 5 pack-years or smoked for the past 2 years; (2) prebronchodilator FEV1% < 60%; (3) diffusing capacity of the lung for carbon monoxide (DLCO) < 80% predicted; (4) asthma exacerbation requiring oral corticosteroids or respiratory tract infection in the past 6 weeks; (5) had been hospitalized for respiratory disease in the past 3 months; and (6) were asthmatic and using more than short-acting β-agonist and/or inhaled corticosteroids (dose equivalent of ≤250 mg fluticasone). General contraindications for MRI also resulted in exclusion from the study.

All individuals participated in 3 separate visits on different days at the same time of the day within ±2 hours (Fig. 1). On the first visit, clinical characteristics were recorded and a physical examination was performed. During this session, DLCO and fractional exhaled nitric oxide (FeNO) were measured, and the Asthma Quality of Life Questionnaire (AQLQ), as well as the Asthma Control Questionnaire (ACQ), was administered.[19] At the second visit (1 week ± 3 days later), subjects returned to the clinic and repeated spirometry, DLCO, AQLQ, FeNO, and sequential sputum induction to more accurately measure these parameters (learning/training effect). At the third and final visit, ^{129}Xe ventilation MRI was performed.

Pulmonary Function Testing

Spirometry, plethysmography, and DLCO were performed using the Vmax Autobox and SensorMedics (CareFusion, San Diego, CA). Spirometry was used to measure FEV1, $FEF_{25\%–75\%}$, and FVC, whereas plethysmography was used to assess lung volumes (total lung capacity [TLC], residual volume [RV]). Ratios such as FEV1/FVC and RV/TLC were calculated from raw data, but all values are reported as percentage of the predicted values for subjects of comparable characteristics. Fractional exhaled nitric oxide, indicating airway inflammation, was measured using the Niox Mino (Aerocrine Inc USA, Morrisville, NC). Asthmatic patients were classified according to the guidelines of the US National Asthma Education and Prevention Program.

Magnetic Resonance Imaging

Hyperpolarized ^{129}Xe MRI scans were performed on a 1.5 T GE Healthcare EXCITE 15M4 MR system. Isotopically enriched ^{129}Xe gas (83% ^{129}Xe) was polarized to 6% to 10% by spin-exchange optical pumping.[20] Subjects underwent 2 fast gradient echo ^{129}Xe ventilation MRI scans in the supine position, 10 minutes apart, using 1 L of total gas volume, composed of 0.5 to 1 L of HP ^{129}Xe, mixed with N_2 buffer gas as described previously.[21] In all cases, the subject received a total volume of gas of 1 L. The xenon volume was determined by the duration of cryogenic accumulation and total gas flow rate. As ^{129}Xe polarization levels became higher, smaller predetermined ^{129}Xe volumes could be used. In case this volume was less than 1 L, helium buffer gas was added to make 1 L.

From each ^{129}Xe MRI scan, VDP was calculated using the linear-binning approach.[22] Subjects were fitted with a flexible chest coil (Clinical MR Solutions, Brookfield, WI) that was tuned to a 17.66-MHz ^{129}Xe frequency and proton-blocked to permit anatomical scans to be acquired using the ^{1}H body coil. After being positioned on the scanner bed, subjects first inhaled a test dose of room air to learn the breathing maneuver. ^{1}H images were acquired in a separate breath hold before the ^{129}Xe scan. For the ^{1}H scans, subjects inhaled 1 L of air from the gas bag to achieve a similar level of lung inflation. Individuals were coached to inhale ^{129}Xe from functional residual capacity. A first bag of gas mixture was used to calibrate the scanner transmit/receive settings

TABLE 1. Sequence Parameters for Thoracic Cavity Registration and the HP ^{129}Xe Ventilation Image

Parameter	Thoracic Cavity ^{1}H Image Steady-State Free Precession Sequence	HP ^{129}Xe Ventilation Image Spoiled Gradient Echo Sequence
Repetition time, ms	2.8	7.9
Echo time, ms	1.2	1.9
Flip angle, degrees	45	5–7
Slice thickness, mm	12.5	12.5
Field of view, cm^2	40 × 40	40 × 28–40
Acquisition matrix	128 × 128	128 × 90–128
Receiver bandwidth, kHz	125	8
Acquisition time, s	15	10–14

in each imaging session. Subjects then underwent 2 HP ^{129}Xe ventilation MRI scans, 10 minutes apart, containing 1 L of total gas volume, composed of 0.5 to 1 L of HP ^{129}Xe, mixed with N_2 buffer gas. The 2 xenon doses were administered to the patient in the supine position. Specific sequence parameters are summarized in Table 1.

Image Analysis

Images were quantified to determine their VDP using a corrected, semiautomated linear-binning approach, first described by He et al.[22] The analysis of the Xe signal was confined to a mask generated by segmenting the proton images to delineate the thoracic cavity. Before segmentation, these images had been registered to the HP ^{129}Xe ventilation MRI scans. Both registration and segmentation by region growing used Avizo (Visualization Sciences Group, Burlington, MA). The HP ^{129}Xe images were then corrected for transmit/receive inhomogeneity and rescaled by the 99th percentile of their cumulative intensity distribution, such that all intensities ranged from 0 to 1. This permitted each ^{129}Xe voxel within the thoracic cavity to be classified into 1 of 4 clusters (<0.2, defect; 0.2–0.4, low intensity; 0.4–0.8, medium intensity; and >0.8, high intensity). The volume of the lowest-intensity cluster (<0.2) relative to that of the thoracic cavity was used to quantify VDP. The 4 clusters representing the HP ^{129}Xe signal intensities within the lungs were color-coded on the ventilation maps: red indicates defect; yellow, low intensity; green, medium intensity; and blue, high signal intensity. Before statistical analysis, the HP ^{129}Xe ventilation images and the corresponding color-coded maps were reviewed in consensus by 2 readers (blinded to the review process, with 6 and 10 years of experience in chest imaging) to verify that image quality was suitable. Image quality was determined to be inadequate for further analysis if the images exhibited extensive coil shading or insufficient signal to noise to undergo binning analysis.

Statistical Analysis

Statistical analysis was performed using JMP 12 (SAS Institute Inc, Cary, NC) and MedCalc 16.1 (MedCalc Software, Ostend, Belgium). Ventilation defect percentage and its change with age were compared between healthy subjects and asthmatic patients using 1-tailed tests; these were justified based on prior knowledge that VDP increases with asthma and age.[23] Correlation between VDP and PFTs was evaluated using the Pearson correlation coefficient (r). Reproducibility of VDP over the 2 consecutive scans was assessed using linear regression, intraclass correlation coefficient, concordance correlation

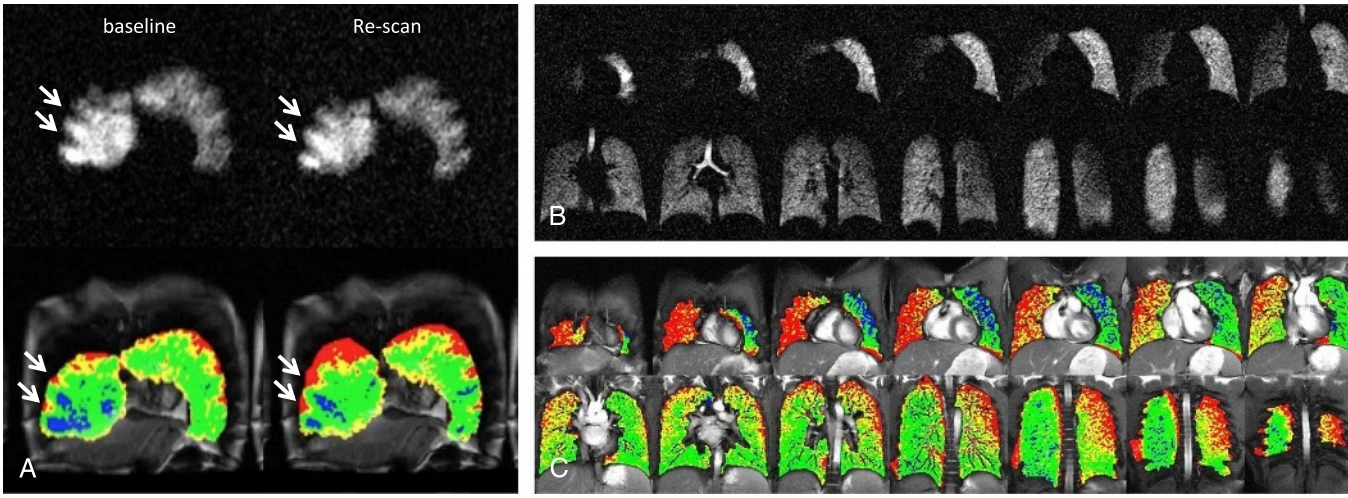

FIGURE 2. Example of false ventilation defects caused by artifacts. A, In this healthy young volunteer, VDP was 7.28% at baseline and 8.33% at second scan. Ventilation defect percentage clusters less than 0.2 (red) were slightly visible at baseline and become more severe at rescan. These defects could be attributed to rib cage impressions (white arrows) representing artifacts. These artifacts were identified during the review and were resolved by manual resegmentation. B, Young asthmatic subject with FEV1% = 80%, which had to be excluded because of extensive coil shading, which caused the binning algorithm (C) to overestimate VDP at 22.4%. Figure 2 can be viewed online in color at www.investigativeradiology.com.

TABLE 2. Summary of the Subject Demographics, Results of the PFTs, and the VDP

	YH (n = 5)	YA (n = 9)	OH (n = 5)	OA (n = 10)
Subject demographics				
Age (±SD), y	23.2 (±1.3)	25.9 (±6.4)	63.4 (±5.8)	63.2 (±6.1)
Male/female	2/3	2/7	2/3	3/7
BMI, kg/m^2	23.7 (±2.5)	29.0 (±8.2)	29.0 (±5.2)	30.3 (±4.1)
ACQ	N/A	1.3 (±0.9)	N/A	1.7 (±1.2)
AQLQ	N/A	6.1 (±0.8)	N/A	5.0 (±1.9)
PFTs				
FEV1%	106 (±14.5)	84 (±16.1)	95.8 (±14.3)	81.1 (±19.8)
FVC%	111.4 (±12.8)	98.8 (±16.2)	104.0 (±18.1)	96.4 (±12.7)
FEV1/FVC	81.0 (±8.2)	72.2 (±7.1)	71.7 (±11.2)	64.5 (±11.2)
$FEF_{25\%–75\%}$	96.2 (±32.3)	59.2 (±21.9)	87.3 (±35.5)	53.1 (±26.9)
RV/TLC	0.18 (±0.02)	0.29 (±0.12)	0.31 (±0.05)	0.40 (±0.05)
DLCO mmol CO	86.8 (±10.5)	97.1 (±10.8)	89.5 (±10.8)	98.4 (±17.3)
FeNO ppb	16.8 (±8.1)	33.8 (±21.4)	15.6 (±10.2)	36.9 (±48.2)
Eos sputum %	4.0 (±5.0)	5.1 (±7.2)	9.3 (±3.4)	5.5 (±3.8)
HP ^{129}Xe MRI				
VDP	5.6 (±1.8)	8.7 (±3.2)	11.6 (±6.6)	16.8 (±10.3)

All values are averages of measurements over 2 time points and are reported as mean ± standard deviation for the cohort.

PFT indicates pulmonary function test; VDP, ventilation defect percentage; YH, young healthy; YA, young asthmatic; OH, old healthy; OA, old asthmatic; BMI, body mass index; ACQ, Asthma Control Questionnaire; AQLQ, Asthma Quality of Life Questionnaire; FEV1%, forced expiratory volume in 1 second; FVC%, forced vital capacity; FEF, forced mid-expiratory flow rate; RV/TLC, residual volume/total lung capacity; DLCO, diffusing capacity of the lung for carbon monoxide; FeNO, fractional exhaled nitric oxide; HP, hyperpolarized; MRI, magnetic resonance imaging; N/A, not applicable.

coefficient,[21] as well as by Bland-Altman analysis. Results were considered statistically significant with $P < 0.05$.

RESULTS

Patients

A total of 30 subjects were enrolled and completed the entire study protocol, with no serious adverse events reported during the imaging sessions. Mild adverse effects related to xenon inhalation (tingling, euphoria, dizziness) resolved within 3 minutes after exhalation. No further adverse effects could be observed. One patient was excluded because the MRI scans were corrupted by shading artifacts, determined to be caused by a malfunctioning coil (Fig. 2). This artifact could not be corrected by retrospective bias field correction due to insufficient signal. This resulted in a final sample size of 29 subjects, of which 19 were mild to moderate asthmatic patients. Pulmonary function test and VDP results are displayed in Table 2.

HP ^{129}Xe MRI Ventilation Defect Analysis

Among all the patients included in the final study cohort, healthy young volunteers yielded the most uniform ^{129}Xe distribution (VDP, 5.6% ± 1.7%; Fig. 3). By comparison, young asthmatic patients exhibited significantly more ventilation defects (VDP, 8.4% ± 3.2%; $P = 0.031$; Fig. 4). Similarly, older asthmatic patients also showed more

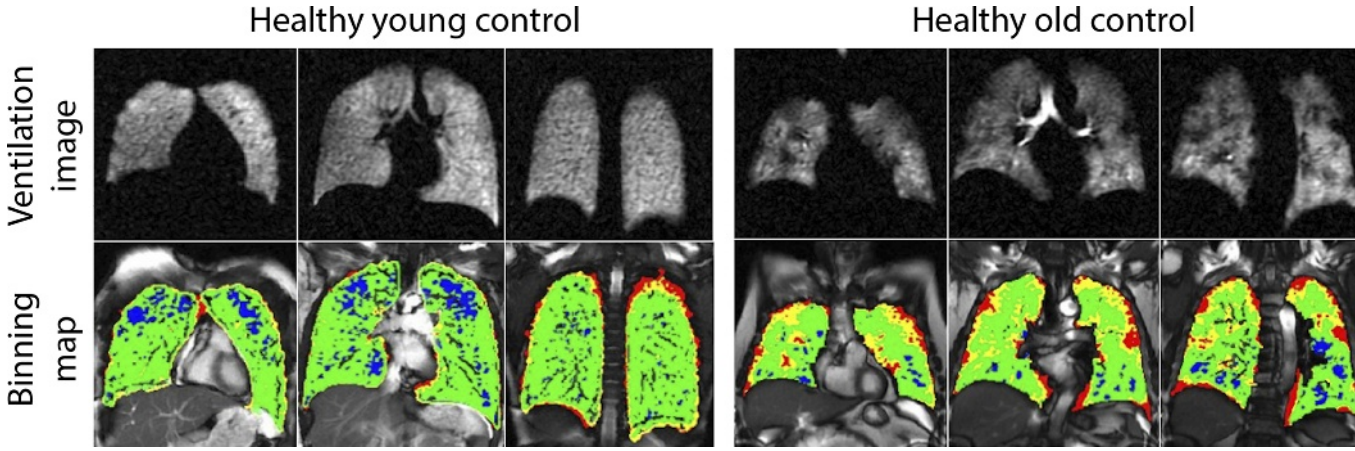

FIGURE 3. Left, Representative HP ^{129}Xe MRI ventilation scan in a healthy young volunteer with FEV1% = 124%. The ^{129}Xe distribution during the breath hold is largely homogeneous. In the corresponding maps, faint red clusters are primarily attributable to slight misregistration, yielding VDP = 3.83%. Right, ^{129}Xe MRI of an older healthy volunteer with FEV1% = 102%. Compared with the young normal, this subject exhibits modest defects in the lung periphery, leading to VDP = 14.4%. Figure 3 can be viewed online in color at www.investigativeradiology.com.

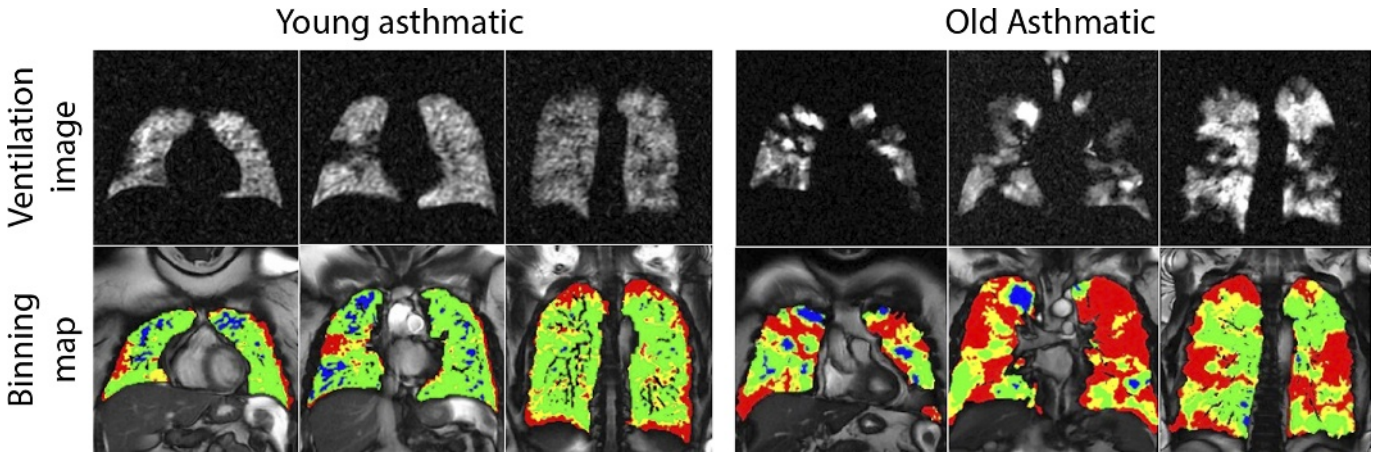

FIGURE 4. Left, Young asthmatic subject; FEV1% = 59%: Moderate ventilation defects are found mainly in the lung periphery and are triangular in shape. On corresponding binning maps, ventilation defects are seen in red, as well as some high signal intensity pixels (blue). VDP: 14.6%. Right, An older asthmatic is depicted on the right; FEV1% = 53%. Scattered ventilation defects are visible throughout the whole lung parenchyma. Both upper and lower lobes, as well as hilar and peripheral lung regions, are almost equally affected. The corresponding VDP maps yielded a total VDP percentage of 44.2%. Figure 4 can be viewed online in color at www.investigativeradiology.com.

defects than older healthy subjects (16.8% ± 10.3% vs 11.6% ± 6.6%; Figs. 3, 4). However, this difference was not significant ($P = 0.13$). Older subjects generally exhibit higher VDP (Fig. 2), and this increase with age was found to be statistically significant (healthy subjects, $P = 0.05$; asthmatic patients, $P = 0.02$) (Table 3).

Comparison of VDP and PFTs

Correlation results are reported in Table 4. Ventilation defect percentage showed a moderate correlation with FEV1% ($r = -0.42$, $P = 0.025$), $FEF_{25\%–75\%}$ ($r = -0.45$, $P = 0.019$), and RV/TLC ($r = 0.51$, $P = 0.0067$), and a strong correlation with FEV1/FVC ($r = -0.70$, $P < 0.0001$; Fig. 5). In addition to PFTs, VDP also correlated strongly with the FeNO ($r = 0.69$, $P < 0.0001$). Ventilation defect percentage did not correlate significantly with FVC, DLCO, ACQ, and the AQLQ questionnaires.

TABLE 3. Parameters

	Healthy vs Asthma		Young vs Old	
Comparison	**Young**	**Old**	**Healthy**	**Asthma**
PFTs				
FEV1%	**0.014**	0.065	0.15	0.36
FVC%	0.069	0.22	0.24	0.36
FEV1/FVC	**0.041**	0.20	0.14	**0.045**
$FEF_{25\%–75\%}$	**0.031**	0.12	0.36	0.30
RV/TLC	**0.014**	**0.042**	**0.020**	**0.018**
DLCO mmol CO	0.060	0.16	0.37	0.42
FeNO ppb	0.036	0.10	0.42	0.57
Eos Sputum %	0.80	0.091	0.063	0.45
HP ^{129}Xe MRI				
Average VDP	**0.031**	0.13	**0.05**	**0.016**

The acquired parameters were tested for significant differences among the healthy and asthma subjects, and also for change with age. Note: significant differences are displayed in bold font-type.

PFT indicates pulmonary function test; FEV1%, forced expiratory volume in 1 second; FVC%, forced vital capacity; FEF, forced mid-expiratory flow rate; RV/TLC, residual volume/total lung capacity; DLCO, diffusing capacity of the lung for carbon monoxide; FeNO, fractional exhaled nitric oxide; HP, hyperpolarized; MRI, magnetic resonance imaging; VDP, ventilation defect percentage.

Repeatability of HP ^{129}Xe VDP and PFTs

The repeatability of VDP proved to be excellent with an intraclass correlation coefficient of 0.977 and concordance correlation coefficient of 0.976 between the 2 MRI scans. Figure 6, A and B, additionally show the results of linear regression and Bland-Altman analysis for VDP. Linear regression yielded an excellent least squares fit for VDP with $R^2 = 0.976$ ($P < 0.0001$). Bland-Altman analysis depicted a small bias (±SD) in VDP of −0.88 ± 1.52, which is largely driven by 2 subjects who had a difference of ~4% between the 2 scans. In contrast, the variability in FEV1% at 1 week was ±183 mL (7.18%) across the subject population, which is well illustrated by the Bland-Altman plot for FEV1% (Fig. 6D).

DISCUSSION

Our study results show that the VDP derived from HP ^{129}Xe MRI is able to detect regional obstruction and significantly correlates with PFTs.

Ventilation defect percentage was moderately to strongly correlated with FEV1%, $FEF_{25\%–75\%}$, FEV1/FVC, and RV/TLC. FEV1% is the predominant metric used for quantitative assessment of airflow limitation in asthma.[24,25] Of note, VDP correlated significantly with FEV1%, $FEF_{25\%–75\%}$, FEV1/FVC, and RV/TLC. However, numerous subjects with normal FEV1% exhibit pronounced ventilation defects, and yet others with abnormal FEV1% exhibit almost normal lung ventilation on MR. This speaks to the different ways these 2 techniques are sensitive to obstruction. In order for HP ^{129}Xe to be detectable in a given voxel, the gas must travel largely unobstructed through all 23 generations of airways. This makes HP ^{129}Xe MRI inherently sensitive to the entire bronchial tree, whereas the measurement of FEV1% is known to be dominated by contributions from the larger airways.[26]

HP ^{129}Xe VDP further correlated with $FEF_{25\%–75\%}$ ($r = -0.45$, $P = 0.019$), which is thought to be a more sensitive indicator of small airways obstruction. This parameter reflects the most effort-independent segment of the spirometric curve, dominated by flow in the small airways. It is here that diseases of chronic airflow obstruction are thought to start, and thus, the correlation of $FEF_{25\%–75\%}$ with HP ^{129}Xe VDP bolsters the notion that VDP is indeed sensitive to small airways obstruction. Because $FEF_{25\%–75\%}$ is known to be less reproducible than

TABLE 4. Correlations of PFTs to VDP

Correlation With VDP	*r*	*P*
FEV1%	−0.42	**0.0249**
FVC%	−0.09	0.6284
FEV1/FVC	−0.71	**<0.0001**
$FEF_{25\%–75\%}$	−0.45	**0.019**
RV/TLC	0.51	**0.0067**
DLCO mmol CO	0.34	0.0858
FeNO ppb	0.69	**<0.0001**
Eos Sputum **%**	0.00	0.9631

Note: significant results are displayed in boldface.

PFT indicates pulmonary function test; VDP, ventilation defect percentage; FEV1%, forced expiratory volume in 1 second; FVC%, forced vital capacity; FEF, forced mid-expiratory flow rate; RV/TLC, residual volume/total lung capacity; DLCO, diffusing capacity of the lung for carbon monoxide; FeNO, fractional exhaled nitric oxide.

FEV1%,[27] HP ^{129}Xe MRI may provide a more reliable metric of small airways obstruction. A finding of potential clinical interest was the strong correlation between VDP and FeNO ($r = 0.69$, $P < 0.0001$), which reflects inflammatory activity and may thus aid in the distinction between young asthmatic patients and young healthy subjects. The sputum eosinophilic count was another recorded measure of airway inflammation; this measure did not correlate with VDP.

The comparison between HP ^{129}Xe VDP and PFTs are relatively virgin ground. To the best of our knowledge, there are only 2 comparable publications addressing the correlations of HP ^{129}Xe VDP and spirometry. In a cohort of COPD subjects, Kirby and coworkers showed a significant correlation between ^{3}He and HP ^{129}Xe MRI VDP, as well as their correlation to FEV1% and FEV1/FVC. In addition, they found that VDP derived from HP ^{129}Xe MRI was significantly higher than from ^{3}He.[28] Kirby and colleagues emphasized that the low density of helium likely makes it less sensitive to obstruction than xenon. To date, the sole study of HP ^{129}Xe MRI in an asthma population was conducted by Svenningsen et al[16] who focused primarily on bronchodilator response and did not report on baseline correlations of HP ^{129}Xe VDP with PFTs.

One cannot overemphasize the need for reproducible markers of airway obstruction. The high degree of variability of FEV1% is one of the major reasons why respiratory clinical trials require large numbers of patients to record an effect. By comparison, the high repeatability observed with HP ^{129}Xe MRI has the potential to mitigate the variability impacting PFTs. We evaluated the repeatability of HP ^{129}Xe MRI by conducting short-term follow-up scans as previously reported with ^{3}He MRI.[29] In particular, the Bland-Altman analysis yielded only a minimal variation of ±1.52%, whereas the variability of FEV1% was found to be ±7.18%. Although the time between FEV1 measurements was considerably longer than for HP ^{129}Xe MRI, such variability is consistent with the known short-term variability of FEV1%.[25,30]

Our study results can have important clinical implications. Measures of VDP with HP ^{129}Xe MRI can be clinically leveraged in monitoring asthma-related changes in ventilation in patients with mild to moderate disease. Supported by the correlation with PFTs and its remarkable repeatability, VDP derived from HP ^{129}Xe MRI could be valuable for the longitudinal assessment of disease progression and therapy response.

Ventilation defect percentage calculation from HP ^{129}Xe MRI is, however, not immune to physiologic states that can potentially hinder the image interpretation. Notably, we observed a substantial overlap in VDP values between old asthmatic patients and age-

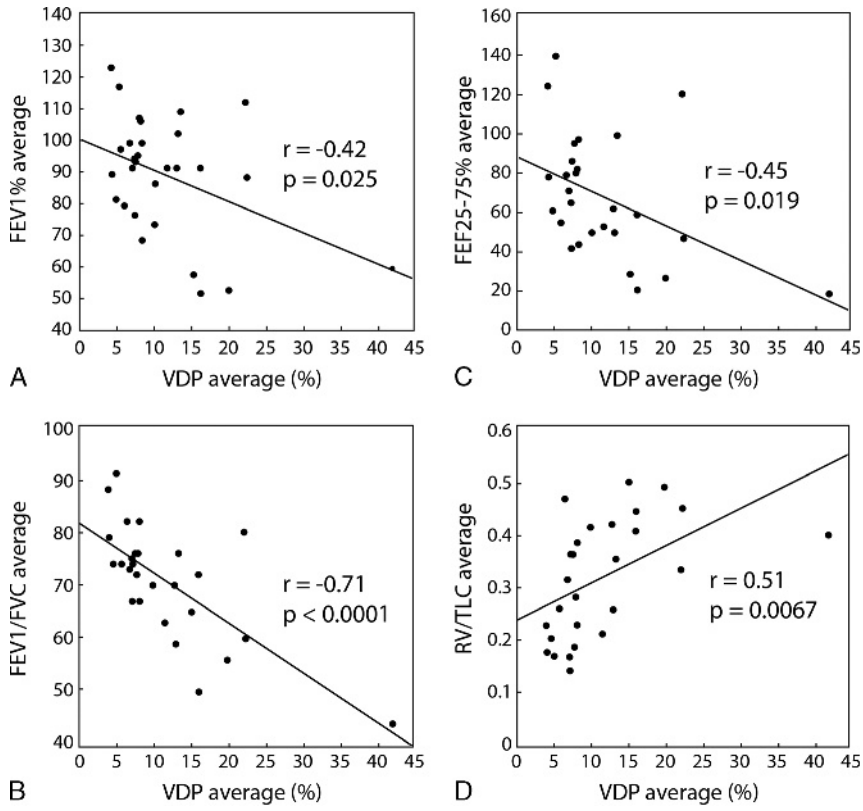

FIGURE 5. Correlation of VDP and FEV1%, $FEV_{25\%-75\%}$, FEV1/FVC, and RV/TLC.

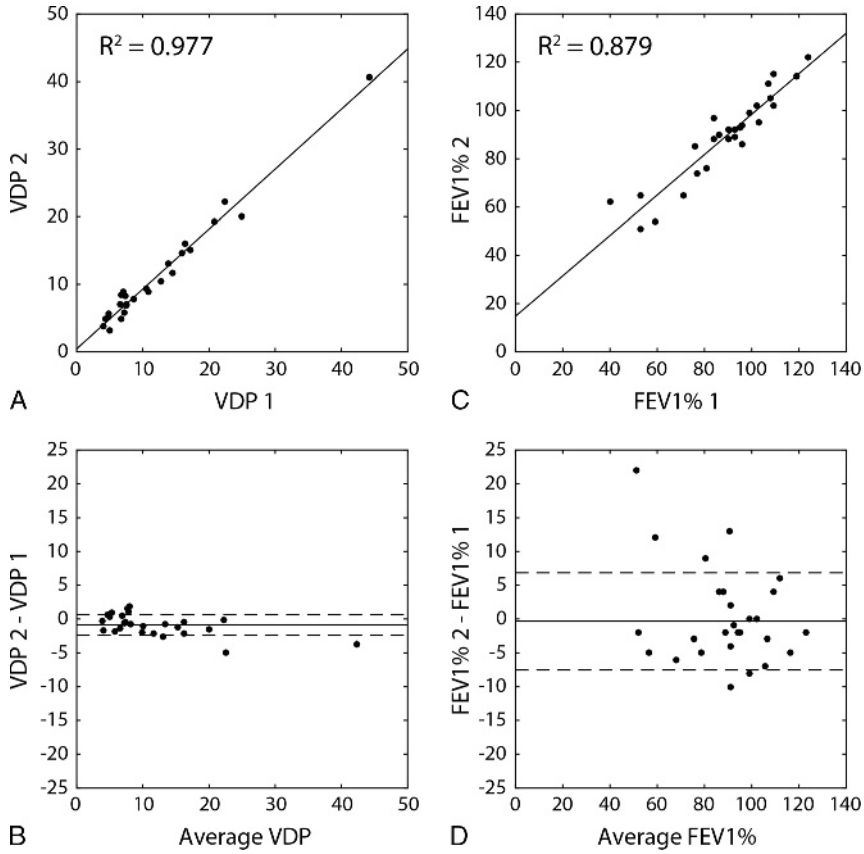

FIGURE 6. Linear regression and Bland-Altman plots for the 2 repeated measures of VDP and FEV1%. Linear regression (A and C) showed high agreement between the 2 scans for VDP (R^2 = 0.976), and slightly lower for FEV1% (R^2 = 0.879). Solid lines indicate the least squared fit. Bland-Altman analysis (B and D) yielded a bias ± SD of –0.88 ± 1.52 for VDP, and –0.33 ± 7.18 for FEV1. Solid line indicates the mean difference and dotted lines indicate the standard deviation about this mean.

matched controls. These subjects could be distinguished by using RV/TLC, which is a marker of changes occurring in the aging lung (ie, senile emphysema).[31,32]

Despite these promising results and possible applications, HP noble gas MRI is not yet used in routine clinical practice. Although the technology (particularly ^{3}He) has been thoroughly studied for 2 decades, it is still limited to selected academic institutions. This can be partially attributed to the complex and nontraditional workflow of HP agents, and the fact that it has not yet been approved by Food and Drug Administration or similar authorities internationally.

Limitations

Our study had notable limitations. Along with the small sample size in the setting of a prospective case-control design, there were differences in the time lapse between repeat measurements of PFTs (ie, 1 week) and MRI (ie, 10 minutes). Thus, the high repeatability of ^{129}Xe MRI observed on short time scales should, in the future, also be verified at longer time scales. In our study, the proton scan and the HP ^{129}Xe ventilation scan were not acquired during the same breath hold owed to the long scan time for each sequence. Consequently, the alignment of the proton images and the ventilation images might not be perfect, potentially leading to artifacts in the binning maps. Future trials could benefit from implementing combined HP gas ventilation images and proton images within a single breath hold.[33] This approach could facilitate the quantification of ventilation defects. Another limitation is represented by the lack of widespread availability of HP noble gas MRI, still to date confined to selected academic institutions. Finally, one could argue that findings from HP ^{129}Xe MRI would further benefit from correlation with other imaging modalities (eg, conventional CT imaging).

In conclusion, our data shows that HP ^{129}Xe MRI is able to quantify airway obstructions in mild to moderate asthma and significantly correlates with PFTs. Its high reproducibility can make this technique a surrogate for PFTs in surveillance of ventilation impairment in asthma patients.

REFERENCES

1. Reed CE. The natural history of asthma. *J Allergy Clin Immunol*. 2006;118:543–548; quiz 549–550.
2. Oraka E, Kim HJ, King ME, et al. Asthma prevalence among US elderly by age groups: age still matters. *J Asthma*. 2012;49:593–599.
3. Bourdin A, Paganin F, Prefaut C, et al. Nitrogen washout slope in poorly controlled asthma. *Allergy*. 2006;61:85–89.
4. Grenier P, Mourey-Gerosa I, Benali K, et al. Abnormalities of the airways and lung parenchyma in asthmatics: CT observations in 50 patients and inter- and intraobserver variability. *Eur Radiol*. 1996;6:199–206.
5. Miller MR, Quanjer PH, Swanney MP, et al. Interpreting lung function data using 80% predicted and fixed thresholds misclassifies more than 20% of patients. *Chest*. 2011;139:52–59.
6. Crapo RO, Casaburi R, Coates AL, et al. Guidelines for methacholine and exercise challenge testing—1999. This official statement of the American Thoracic Society was adopted by the ATS Board of Directors, July 1999. *Am J Respir Crit Care Med*. 2000;161:309–329.
7. Roos JE, McAdams HP, Kaushik SS, et al. Hyperpolarized gas MR imaging: technique and applications. *Magn Reson Med*. 2016;75:1434–1443.
8. Kong X, Sheng HX, Lu GM, et al. Xenon-enhanced dual-energy CT lung ventilation imaging: techniques and clinical applications. *AJR Am J Roentgenol*. 2014;202:309–317.

9. Renne J, Hinrichs J, Schönfeld C, et al. Noninvasive quantification of airway inflammation following segmental allergen challenge with functional MR imaging: a proof of concept study. *Radiology*. 2015;274:267–275.
10. Kruger SJ, Fain SB, Johnson KM, et al. Oxygen-enhanced 3D radial ultrashort echo time magnetic resonance imaging in the healthy human lung. *NMR Biomed*. 2014;27:1535–1541.
11. Halaweish AF, Moon RE, Foster WM, et al. Perfluoropropane gas as a magnetic resonance lung imaging contrast agent in humans. *Chest*. 2013;144:1300–1311.
12. Altes TA, Powers PL, Knight-Scott J, et al. Hyperpolarized ^{3}He MR lung ventilation imaging in asthmatics: preliminary findings. *J Magn Reson Imaging*. 2001; 13:378–384.
13. de Lange EE, Altes TA, Patrie JT, et al. Evaluation of asthma with hyperpolarized helium-3 MRI: correlation with clinical severity and spirometry. *Chest*. 2006;130: 1055–1062.
14. Tzeng YS, Lutchen K, Albert M. The difference in ventilation heterogeneity between asthmatic and healthy subjects quantified using hyperpolarized ^{3}He MRI. *J Appl Physiol*. 2009;106:813–822.
15. Costella S, Kirby M, Maksym GN, et al. Regional pulmonary response to a methacholine challenge using hyperpolarized (3)He magnetic resonance imaging. *Respirology*. 2012;17:1237–1246.
16. Svenningsen S, Kirby M, Starr D, et al. Hyperpolarized (3) He and (129) Xe MRI: differences in asthma before bronchodilation. *J Magn Reson Imaging*. 2013;38: 1521–1530.
17. Fain SB, Gonzalez-Fernandez G, Peterson ET, et al. Evaluation of structure-function relationships in asthma using multidetector CT and hyperpolarized He-3 MRI. *Acad Radiol*. 2008;15:753–762.
18. Kirby M, Svenningsen S, Owrangi A, et al. Hyperpolarized ^{3}He and ^{129}Xe MR imaging in healthy volunteers and patients with chronic obstructive pulmonary disease. *Radiology*. 2012;65:600–610.
19. Koshak EA. Classification of asthma according to revised 2006 GINA: evolution from severity to control. *Ann Thorac Med*. 2007;2:45–46.
20. Driehuys B, Cates GD, Miron E, et al. High-volume production of laser-polarized Xe-129. *Appl Phys Lett*. 1996;69:1668–1670.
21. He M, Robertson SH, Kaushik SS, et al. Dose and pulse sequence considerations for hyperpolarized ^{129}Xe ventilation MRI. *Magn Reson Imaging*. 2015;33: 877–885.
22. He M, Kaushik SS, Robertson SH, et al. Extending semiautomatic ventilation defect analysis for hyperpolarized (129)Xe ventilation MRI. *Acad Radiol*. 2014;21: 1530–1541.
23. Svenningsen S, Kirby M, Starr D, et al. What are ventilation defects in asthma? *Thorax*. 2014;69:63–71.
24. Nair P, Dasgupta A, Brightling CE, et al. How to diagnose and phenotype asthma. *Clin Chest Med*. 2012;33:445–457.
25. Miller MR. Standardisation of spirometry. *Eur Respir J*. 2005;26:319–338.
26. van der Wiel E, Hacken NHT, Postma DS, et al. Small-airways dysfunction associates with respiratory symptoms and clinical features of asthma: a systematic review. *J Allergy Clin Immunol*. 2013;131:646–657.
27. Ciprandi G, Capasso M, Tosca M, et al. A forced expiratory flow at 25-75% value <65% of predicted should be considered abnormal: a real-world, cross-sectional study. *Allergy Asthma Proc*. 2012;33:5–8.
28. Kirby M, Svenningsen S, Owrangi A, et al. Hyperpolarized ^{3}He and ^{129}Xe MR imaging in healthy volunteers and patients with chronic obstructive pulmonary disease. *Radiology*. 2012;265:600–610.
29. Mathew L, Evans A, Ouriadov A, et al. Hyperpolarized ^{3}He magnetic resonance imaging of chronic obstructive pulmonary disease: reproducibility at 3.0 Tesla. *Acad Radiol*. 2008;15:1298–1311.
30. Reddel HK, Taylor DR, Bateman ED, et al. An Official American Thoracic Society/European Respiratory Society Statement: Asthma Control and Exacerbations. *Am J Respir Crit Care Med*. 2009;180:59–99.
31. Janssens JP, Pache JC, Nicod LP. Physiological changes in respiratory function associated with ageing. *Eur Respir J*. 1999;13:197–205.
32. Parraga G, Mathew L, Etemad-Rezai R, et al. Hyperpolarized ^{3}He magnetic resonance imaging of ventilation defects in healthy elderly volunteers: initial findings at 3.0 Tesla. *Acad Radiol*. 2008;15:776–785.
33. Horn FC, Tahir BA, Stewart NJ, et al. Lung ventilation volumetry with same-breath acquisition of hyperpolarized gas and proton MRI. *NMR Biomed*. 2014; 27:1461–1467.